

New Method for Measuring Crack Propagation in Asphalts

J.M. READ*

Senior Asphalt Development Engineer, Shell Bitumen UK, Riversdell House, Guildford Street, Chertsey, Surrey, England KT16 9AU

(Received February 3, 1999; Revised September 8, 1999)

This paper describes the development of a novel method of measuring the rate of crack propagation in asphalt mixtures using image analysis techniques. The techniques developed incorporate methods to observe the crack more clearly as well as a semiautomatic analysis of the images taken during 3 point bend tests on beams of asphalt. The results show that modified binders increase the resistance to crack propagation and that the path of least resistance to cracks appears to be the interface between the coarse aggregate and the matrix

In addition a model is presented for both polymer modified and unmodified asphalts for calculating the effect of crack propagation on analytical design techniques. The model developed is based around the 3 point flexure of beams of asphalt and monitoring the degradation of load (stiffness) with time.

Keywords: Crack, Propagation, Asphalt, Image analysis, Stiffness

INTRODUCTION

Once crack initiation has taken place in a bituminous road layer the pavement is still capable of sustaining traffic loading. Crack initiation is followed by a period of crack propagation which can be significantly longer than the time required to initiate a crack (Brunton, 1989). Therefore, crack propagation is an extremely important phenomenon which needs to be assessed and, if possible, quantified as it is the cracks, when propagated, which cause weakening of the pavement structure. To do this in-situ, as with all fatigue characterisation, is very difficult, hence, surrogate testing methods are needed. Two generic methods have been adopted in previous research; a

theoretical approach, based on fracture mechanics (extensively developed with research into metals), and a practical experimental approach, simulating crack propagation. Both methods have merit, but for the purposes of this research it was decided to carry out simulative testing, due to the inherent difficulties encountered by a number of researchers (Krans 1993, Majidzadeh *et al* 1973 and Molenaar 1983) when using fracture mechanics for a 2 or 3 phase bituminous material instead of for continuous material for which the theory was developed.

The test method developed for this project is shown schematically in Figure 1 and a photograph is given in Plate 1. It was developed from apparatus used in previous research into reflective cracking (Caltabiano,

* John.M.Read@ope.shell.com

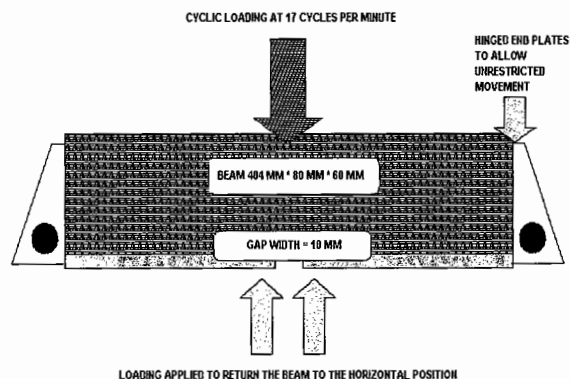


FIGURE 1 Schematic showing the test configuration for crack propagation



PLATE 1 Beam cracking apparatus

1990) and used a beam of material with two steel plates glued to the bottom. A 10mm gap was left between the plates to act as a crack initiator and the beam was supported at both ends and hinged to allow flexure to take place without imposing restrictive forces. Load was applied via a pneumatic actuator situated above the beam directly above the gap in the steel plates with a second actuator beneath the beam to return it to the normal position after each load pulse.

The system was controlled by computer to apply the load using a pseudo-sinusoidal waveform. The controlling parameter was the strain measured across

the gap between the steel plates. The displacement, over the gauge length of 10mm, was monitored using Linear Variable Differential Transformer's (LVDT's) mounted on either side of the beam, the outputs of which were averaged and the value used for the control of the test. The crack that developed on the surface of the beam, as the test progressed, was photographed using a computer controlled camera and these images were then analysed using state-of-the-art image analysis equipment and software. The crack was made more visible by application of white paint to the surface of the beam. The second form of analysis examined the fall off of load as the test progressed. It was decided to stop the test once the load reached 25% of its' original value, as little change occurred after this reduction due to the crack tip approaching the neutral axis of the beam. The level of strain across the gap in the steel plates, in the main test programme, was 8,500 microstrain. This value was selected, after analysis of the specimens tested in the pilot programme, because the average length of test for each specimen was required to be of the order of 24 hours in order to complete the main test program in the time available. The number of load applications to failure, as defined above, then allowed a ranking of the materials and assessment of the material parameters which had an effect on the resistance to crack propagation.

IMAGE ANALYSIS

Image analysis equipment was used as one method of determining the rate of crack propagation. The equipment was used to analyse photographs of the beams, which were taken at specific reductions in the stiffness (100%, 90%, 80%, 70%, 60%, 50%, 45%, 40%, 35%, 30% and 25% of the original stiffness) of the beam showing varying stages of cracking, and consisted of:

- A high quality servo-controlled CCD camera, the functions of which (focus, zoom, aperture and iris) were controlled via the computer. The camera had the red, green and blue colours on separate chips

allowing exceptionally high quality images to be obtained for subsequent analysis.

- A digital frame grabber, installed in the computer, which digitised the image received from the camera. The controlling software for the frame grabber also allowed some manipulation of the image (sharpening, smoothing, Fourier transforms etc.) in order to ensure the correct image was obtained prior to analysis.
- A high specification graphics computer which allowed high speed processing, essential as each image contained up to 8Mb of information. The computer had a specially designed monitor which had the resolution required for the high quality images produced by the camera.

The software obtained for use with the above system was a state-of-the-art package capable of processing and analysing in excess of thirty images at the same time. Therefore, processing and analysing all the images from one specimen was able to be done at the same time, reducing work and increasing the speed of analysis. Some additional software was also obtained which allowed the processed images to be annotated and to be exported to PC based systems.

The overall system, as described above, allowed the measurement of the true crack length on the surface of the beam, as opposed to the methods which have been applied previously (Caltabiano, 1989 and Krans *et al*, 1993). These only measured the linear distance the crack had travelled and did not take into account the actual distance, Figure 2. It was, therefore, expected that this novel method of crack length measurement would allow a better assessment of the true rate of crack propagation in the test specimens.

PILOT TEST PROGRAMME

This was carried out to investigate the test parameters and conditions which should be used for the main test programme. It consisted of testing eighteen beams of a 20mm Dense Bitumen Macadam (DBM) (BS 4987, 1993). This material was chosen as it was expected that it would have crack propagation properties some-

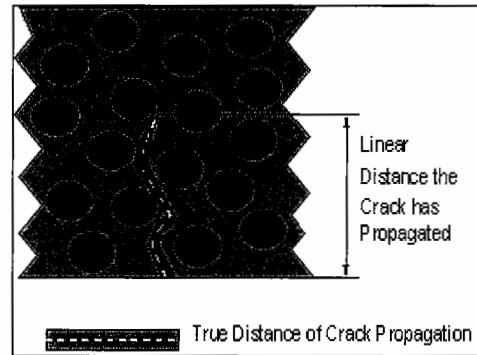


FIGURE 2 Schematic showing that the true distance of crack propagation is longer than the linear distance measured by previous research

where between those of the other two mixtures to be evaluated.

The test parameters and conditions evaluated were:

- Method of test control (stress, strain or crack opening),
- Strain level,
- Temperature susceptibility,
- Method of volumetric measurement (sealed, unsealed and geometric),
- Beam geometry,
- Method of image capture and storage and
- Method of monitoring the position of the crack.

RESULTS OF THE PILOT TEST PROGRAMME

Evaluating the method of test control was carried out prior to the pilot test programme (Bolton, 1994). After reviewing the available literature and carrying out some validation tests, the method of control considered most suitable was the strain developed across the gap between the steel plates. The deflection across the gauge length of 10mm was sufficiently large to measure accurately and the LVDT's were easy to position. The beam geometry was investigated and a beam 404mm long with an 80mm square section was found suitable. All beams were sawn from a slab of material

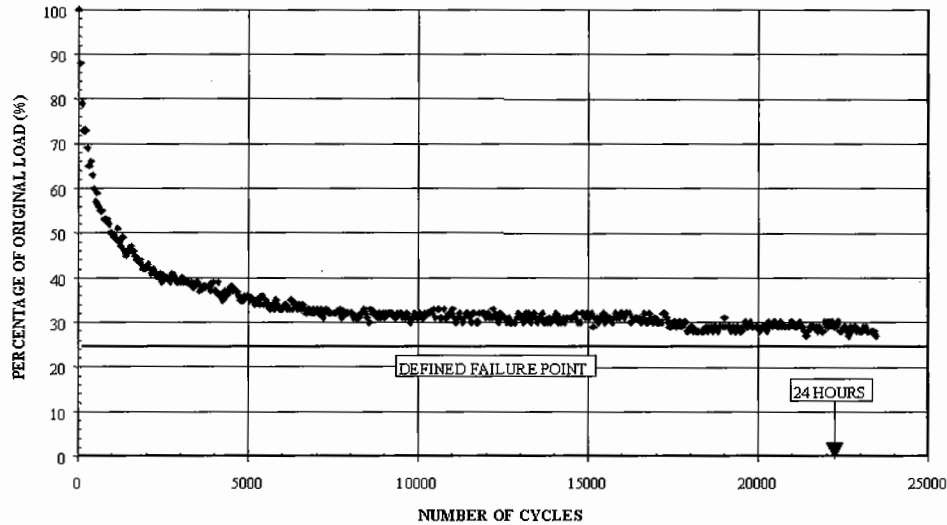


FIGURE 3 Typical beam tested at 7,500 microstrain

404 × 280 × 127mm produced in accordance with a strict protocol (Read 1996).

The average level of applied strain, in order to fail the beams, on average, in 24 hours, was 8,500 microstrain. Figure 3 shows results from a test at 7,500 microstrain indicating that the failure condition had not been reached in 24 hours. By contrast, Figure 4 demonstrates that the chosen level of strain (8,500 microstrain) fails the beam within an acceptable time period. The need to fail the beams within 24 hours was due to time constraints on the research and did result in a level of strain which would never be seen in a conventional pavement. To this end there is a need to extend the research to ascertain if extrapolation of the high strain data to realistic strain conditions is valid. Initially the testing apparatus was not temperature controlled and it was found that this led to a high variability in the response of the beams to the applied load, as would be expected for a visco-elastic plastic material. Therefore, the decision was taken to house the apparatus inside a temperature controlled room. Testing was then carried out at 0°C, 10°C and 20°C (these temperatures were chosen due to the constraints of the heating and cooling system

used in the temperature controlled room) and this indicated that temperature influenced the magnitude of the difference between results but did not change the ranking and, hence, all further testing was carried out at 20°C. This prevented further variability in the results due to temperature.

The method of volumetric measurement was investigated, as the work involved in sealing the 216 beams from water ingress, for the main test programme, prior to density measurement and stripping them afterwards, was considerable (approximately 1 hour per beam). It was hoped that accurate geometric measurements, on a large specimen, would allow the calculation of the density with an acceptable accuracy. However, the differences between the three proposed methods was large and it was, therefore, decided that all the density measurements would have to be carried out using the sealed method.

The majority of the beam tests, in the pilot study, were used to ascertain how best to capture images, at what rate and under what lighting conditions. The ideal method of capturing the images would have been to use the image analysis equipment controlled by the same computer as the test itself. This was not

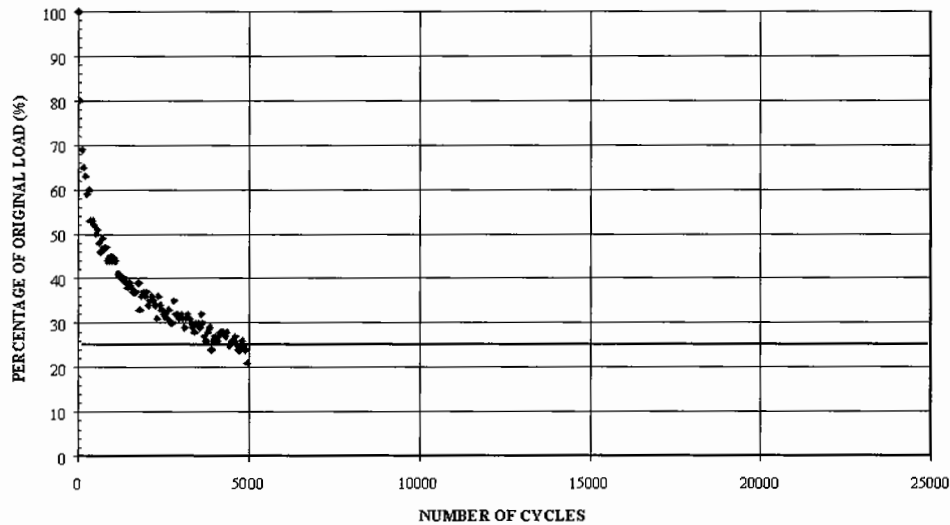


FIGURE 4 Typical beam tested at 8,500 microstrain

feasible as it would have required sole use of the image analysis equipment which had demands from other research projects. Therefore, a high quality camera, with a databack for image referencing, was used. The rate of image capture was chosen to be 12 photographs per beam as this allowed the three replicates of each beam type to be stored on one film (36 exposure). The lighting conditions proved to be the greatest problem as external lighting, needed at fast shutter speeds, raised the temperature of the beam, interfering with the temperature control. To overcome this, the background lighting in the temperature controlled room was made as bright as possible, while the beam was placed as far from the external light source as was practical. After many attempts, an appropriate configuration, aperture, shutter speed and level of background illumination was achieved which provided clear, sharp and bright images suitable for image analysis, an example of which is shown in Plate 2 (subsequently several samples were evaluated to check the repeatability of this method which was found to be acceptable, however, it was not possible to place numbers on the repeatability as the assessment at this point was purely qualitative). Monitoring

the crack also proved to be a difficult problem. In order to observe the crack clearly a suitable coating for the beam was required. Various white coatings were tried and the best was found to be a car priming paint. This did not shatter as both Plaster of Paris and whitewash did and did not disguise crack growth, as polymer modified paints did. The car priming paint was applied by aerosol allowing a good surface finish to be obtained.

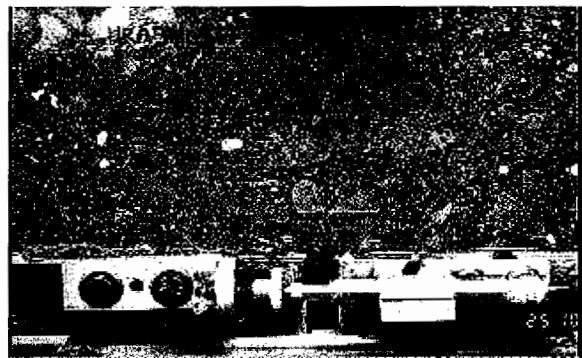


PLATE 2 Digitised image of beam prior to application of white paint and testing

MAIN TEST PROGRAMME

The main test programme was designed to determine which material properties affect the resistance to crack propagation in a bituminous mixture.

Three material types were selected:

- Hot Rolled Asphalt – 30/14 (HRA) – Mid specification grading (BS 594, 1992),
- Dense Bitumen Macadam – 20mm (DBM) – Mid Specification grading (BS 4987, 1993) and
- Heavy Duty Macadam – 40mm (HDM) – Mid specification grading (BS 4987, 1993).

Four binder types were selected:

- 50 pen,
- 100 pen,
- SBS modified bitumen supplied pre-blended (Carphalte DM) and
- EVA modified bitumen supplied pre-blended (Evaphalte).

Three binder contents were selected:

- Optimum^{Note 1} less one percent,
- Optimum and
- Optimum plus one percent.

Note 1 Optimum is defined as the Marshall optimum for the HRA and as the middle of the British Standard for the two continuously graded mixtures.

Two void contents were selected:

- A void content in the middle of the normal operating range and
- A high void content 2% above the middle of the operating range.

These various combinations entailed the manufacture of 72 slabs of material with 3 beams (replicate testing) being taken from each slab. Thus, there were 216 beams to manufacture and test. These beams were tested under the experimental conditions described previously. Each beam was uniquely referenced using a 7 digit code made up as follows:

HRA 5 L L 1

The first 3 letters refer to the mixture type:

HRA	Hot Rolled Asphalt
DBM	Dense Bitumen Macadam

The next character refers to the type of bitumen:

5	50 pen
1	100 pen
E	EVA modified
S	SBS modified

The next letter refers to the void content:

H	High void content
L	Low void content

The next letter refers to the binder content:

H	Optimum plus 1%
O	Optimum
L	Optimum minus 1%

The last number refers to the replicate number:

1	First replicate
2	Second replicate
3	Third replicate

Figures 5, 6 and 7 are shown here to demonstrate that the method of testing was appropriate. They also show that beam 2 of each set of replicates generally gave longer lives than the other two. Beam 2 was the centre beam cut from the slab and as such was not subject to edge restraints during compaction. Therefore, the aggregate structure was allowed to find its preferred orientation. The two outside beams were subject to restraint from the mould which, it is thought, affected the particle structuring. In an ideal world the slab from which the beams were cut would have been much larger negating the effect of edge restraint. However, the practicalities of doing this were such as to make it totally impractical and, hence, the method stated above was used.

Plate 3 shows a digitised image of the beam in Plate 1, coated with primer with a crack through it. Plate 4 shows the ability of the image analysis system, as the crack has been superimposed onto the uncoated

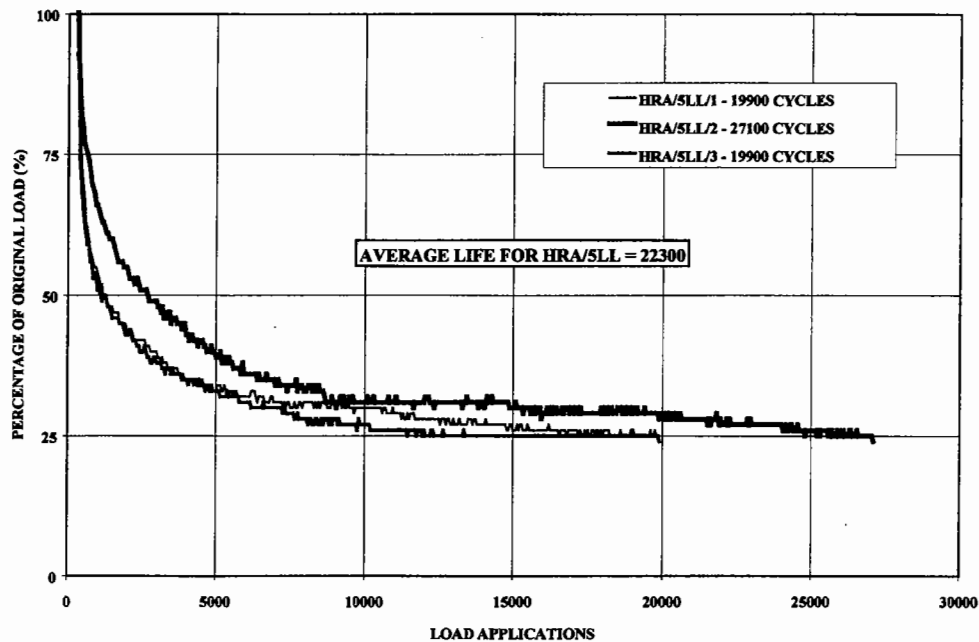


FIGURE 5 Beam test result for specimens HRA/5LL – Hot Rolled Asphalt, 50 pen bitumen, low void content and low binder content

image. This allows the path taken by the crack to be analysed, which was not previously possible.

The main test programme described here was streamlined due to the extremely high performance, long test time, of the SBS modified materials (Cariphalte DM). This streamlining meant that only two material types were evaluated (HRA and DBM) and for the majority of the polymer modified materials only one out of the three beams manufactured was tested (beam 2). Although it would have been desirable to have completed the test programme as planned the data still had the following variations for the unmodified materials:

- Two materials types (30/14 HRA and 20mm DBM),
- Two bitumen types (50pen and 100pen),
- Three binder contents (optimum, optimum +1% and optimum -1%),
- Two compaction levels (normal and normal +2%) and
- Three replicates of each material.

which gave 24 different mixtures and 71 beams (1 beam failed prematurely due to a power surge) and for the polymer modified materials:

- Two materials types (30/14 HRA and 20mm DBM),
- Two bitumen types (SBS {Cariphalte DM} and EVA {Evaphalte} modified),
- Three binder contents (optimum, optimum +1% and optimum -1%),
- Two compaction levels (normal and normal +2%) and
- Generally one beam of each material.

which gave 16 different mixtures and 23 beams as not all of the combinations were evaluated:

Therefore, this gave a total of 40 different mixtures and 112 beams: 94 from the main test programme with 18 beams from the pilot test programme.

RESULTS OF THE MAIN TEST PROGRAMME

Image analysis

It was hoped that the use of image analysis to measure the cracks would produce a new way to quantify

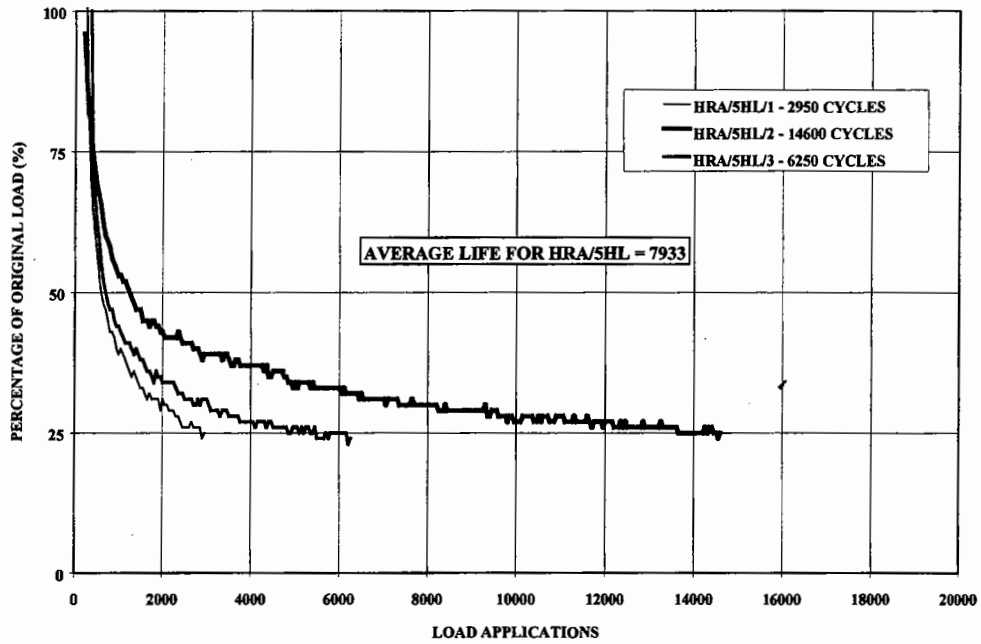


FIGURE 6 Beam test result for specimens HRA/5HL – Hot Rolled Asphalt, 50 pen bitumen, high void content and low binder content

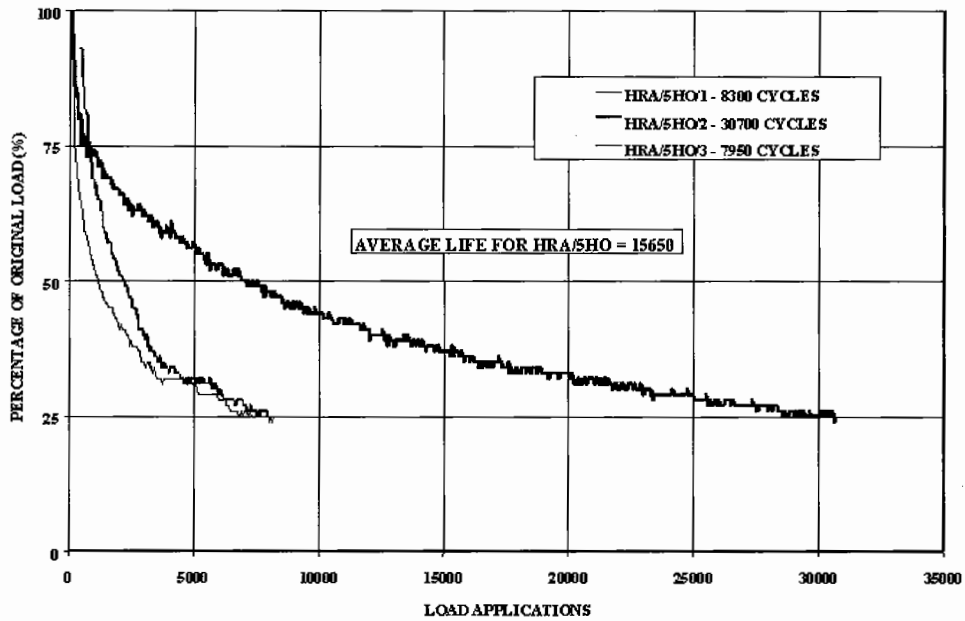


FIGURE 7 Beam test result for specimens HRA/5HO – Hot Rolled Asphalt, 50 pen bitumen, high void content and optimum binder content

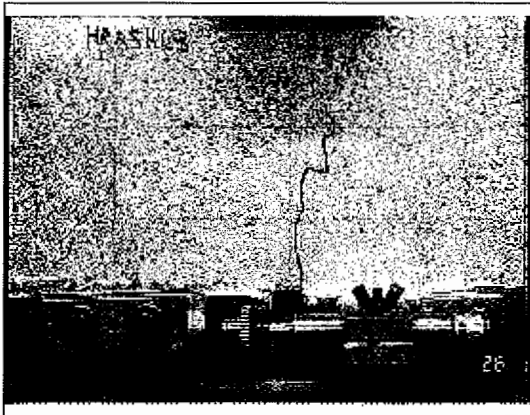


PLATE 3 Digitised image of a beam – after testing

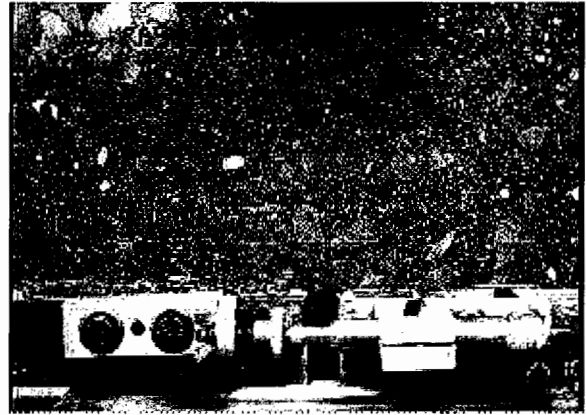


PLATE 4 Digitised image of the beam in Plate 3 with the crack electronically superimposed – showing the path taken around the aggregate structure

crack propagation rates. This was not possible, however, as only about 50 of the beams tested had visible cracks, with no measurable cracks apparent on any of the polymer modified beams which at this point is a unfortunate limitation of the analysis method. Typical graphs and Plates are given in Figures 8 to 10 and Plates 5 to 7. These show very clearly that the method has potential but that further work into this area is required, particularly in monitoring polymer modified mixtures. Measurement of the true crack length is considered worthwhile as it should allow a new definition of failure in future testing since it is this parameter which the author considers has given rise to much of the variation in the data shown later in this paper. This method has also shown, by the electronic superimposition of the crack onto the unpainted beam, the way in which cracks grow and which route they take. By examining all the images it is clear that cracks tend to propagate around the coarse aggregate passing as close to the aggregate as possible. The cracks also try and travel the shortest route between the point of crack initiation and the point of applied load.

These findings suggest the need for future work where, it is envisaged, the route of propagation will be predicted, by the use of image analysis, prior to the test taking place. As it is considered that a crack will always take the weakest path, the results would imply that the interface between the aggregate and the matrix is less resistant to cracking than the matrix

(cracks are unlikely to propagate through the coarse aggregate). Therefore, the lower the amount of coarse aggregate the better and, hence, this partially explains the better performance of gap graded materials in comparison to continuously graded ones. However, if a continuously graded material is to be used then the higher the quantity of coarse aggregate the better as it makes the propagation route of the crack longer, thus, increasing the life.

Further work is required on the use of image analysis in crack propagation work, particularly in the control of the test, the definition of failure and to monitor the progression of cracks in real time.

Analysis of crack propagation data

When analysing the data it became clear that one important parameter of the mixture, with regard to crack propagation, was stiffness. The stiffness of the beams was ascertained by comparing the magnitude of the initial load with stiffness data from indirect tensile testing on cylindrical specimens (BS DD 213, 1993) of the same material carried out prior to the main test programme. This resulted in a good correlation and although the applied stress was significantly higher in the beam tests than that applied during the stiffness tests, both values of stress were in the area

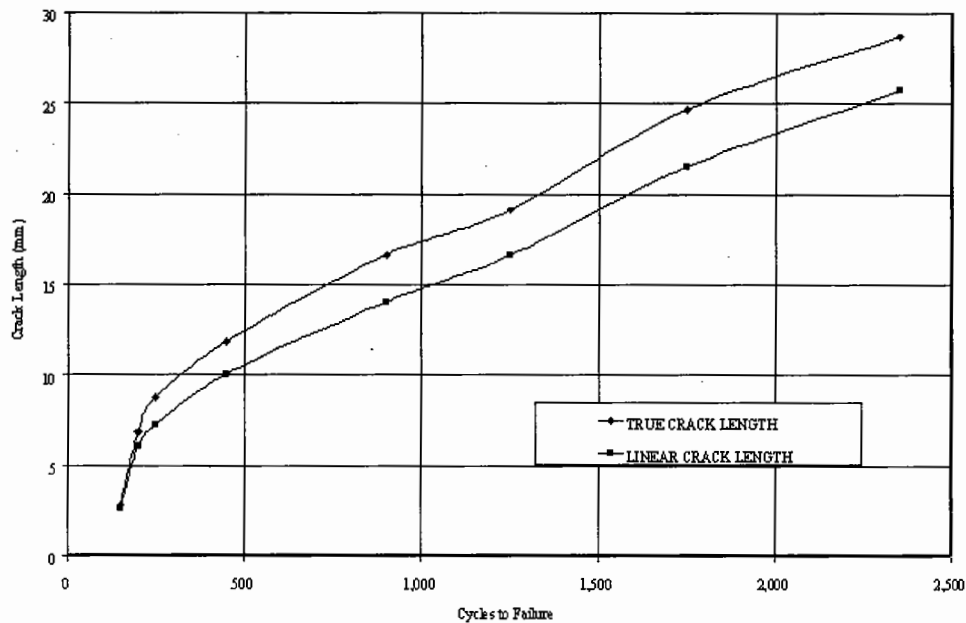


FIGURE 8 Rates of crack growth for specimen HRA5HH3 showing both the linear and the true crack lengths

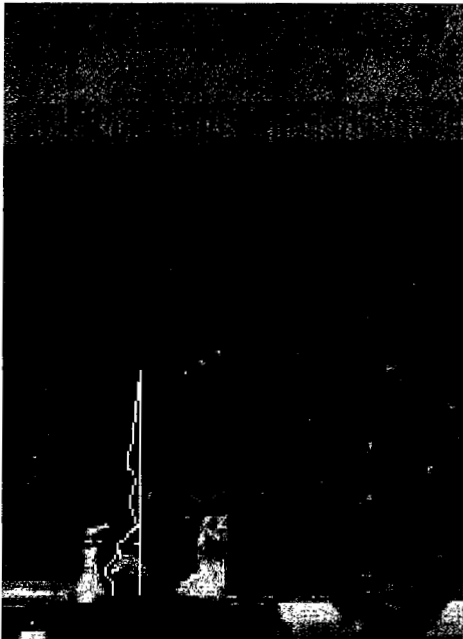


PLATE 5 Electronically superimposed crack on unpainted beam - specimen HRA5HH3 (See Color Plate I at the back of this issue)

where the stiffness is much less dependent on the level of stress applied (Read 1996). Hence, it was considered that this was an acceptable method of estimating the stiffness of the beams.

During the main test programme many variables were examined but none of these could explain the variations in performance found during the testing. However, each of the variables did have an influence on the stiffness which in turn was able to explain the variation in performance. The data when presented in the form of stiffness against number of cycles to failure fell into four distinct groups:

- Unmodified HRA,
- Unmodified DBM,
- SBS modified mixtures (Cariphalte DM) and
- EVA modified mixtures (Evaphalte).

These results are presented in Figures 11 to 15. It can be seen that crack propagation appears to be related to the stiffness of the mixture in a power relationship. The equations of the 4 best fit lines are given in Equations 1 to 4 and these all indicate that the

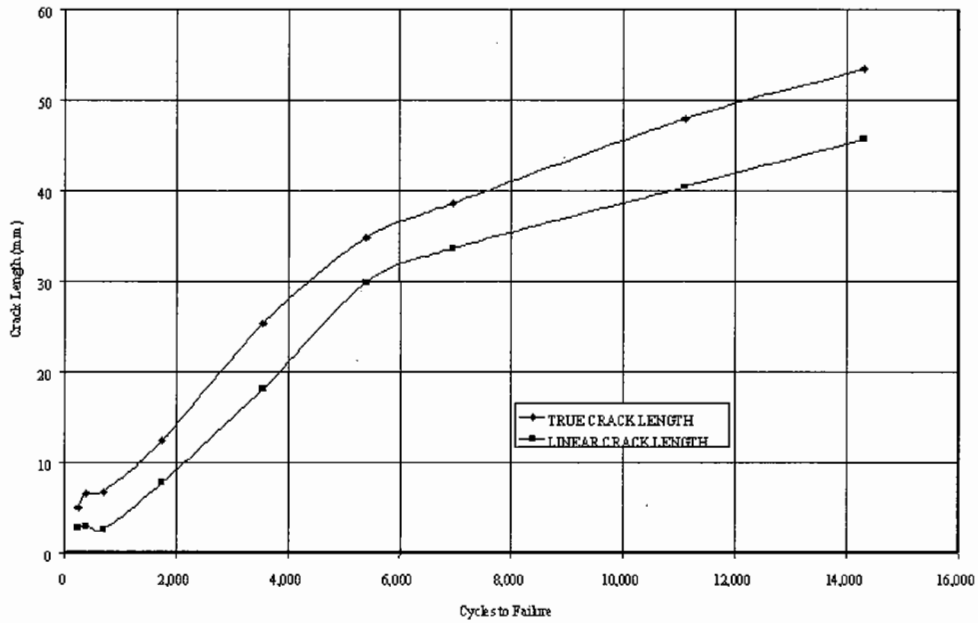


FIGURE 9 Rates of crack growth for specimen HRA5HH1 showing both the linear and the true crack lengths

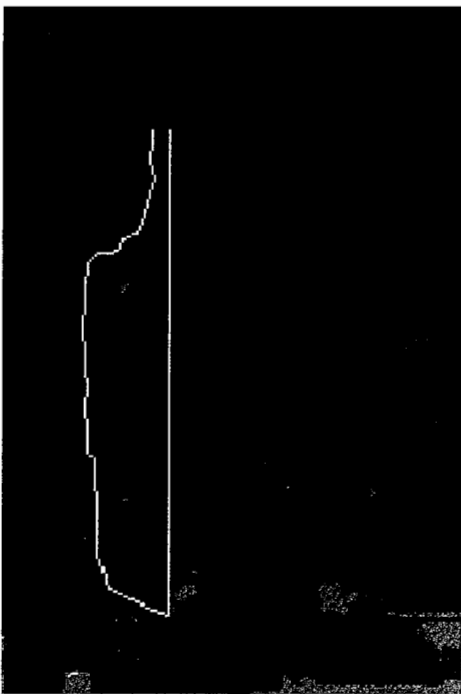


PLATE 6 Electronically superimposed crack on unpainted beam - specimen HRA5HH1 (See Color Plate II at the back of this issue)

lower the stiffness of a bituminous mixture the better its resistance to crack propagation. This is in direct contradiction to the requirements for prevention of crack initiation in a thick bituminous pavement but in agreement for a thin bituminous pavement.

$$\text{Unmodified DBM } N = \left(\frac{S_m}{6563} \right)^{-8.482} \quad (1)$$

$$\text{Unmodified HRA } N = \left(\frac{S_m}{16843} \right)^{-5.063} \quad (2)$$

$$\text{SBS Modified } N = \left(\frac{S_m}{138380} \right)^{-2.548} \quad (3)$$

$$\text{EVA Modified } N = \left(\frac{S_m}{6101} \right)^{-7.770} \quad (4)$$

Where :

N = Number of cycles to failure

S_m = Stiffness modulus at 20°C and a risetime of 120ms or frequency of 1.3 Hz.

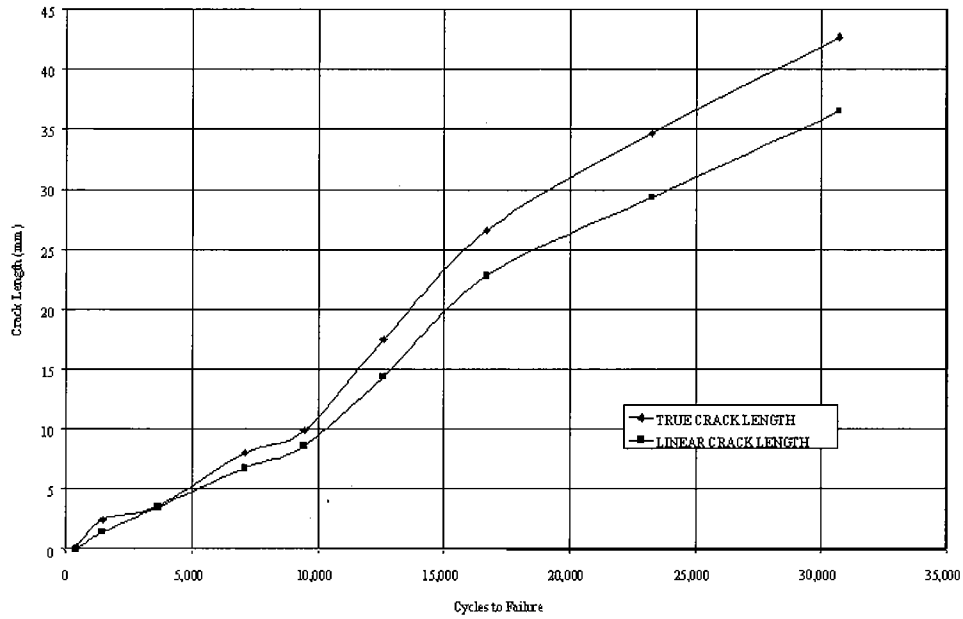


FIGURE 10 Rates of crack growth for specimen HRA5HO2 showing both the linear and the true crack lengths

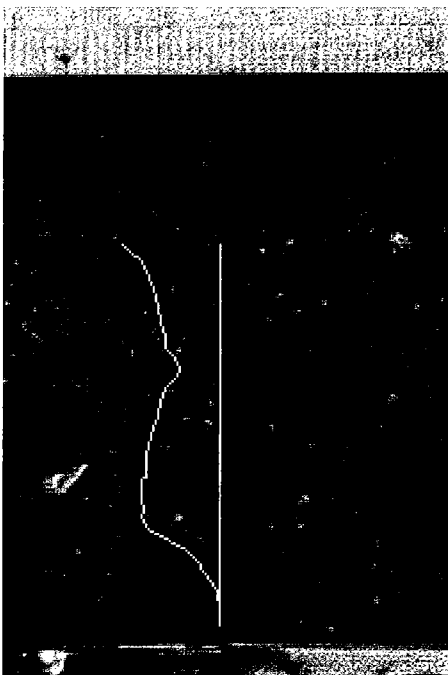


PLATE 7 Electronically superimposed crack on unpainted beam - specimen HRA5HO2 (See Color Plate III at the back of this issue)

These four equations allow calculation of the number of cycles for crack propagation, for any material encompassed in the range of mixtures tested, provided that an appropriate value of stiffness modulus is available for the material. This will, in turn, allow a design shift factor for crack propagation for the material to be developed provided one material is selected as the datum to which all others are compared. This work on a shift factor is shown in the next section of this paper and demonstrates that the research has advanced the way in which crack propagation can be treated in pavement design and evaluation. However, it is important to reiterate that the equations are only valid for the conditions under which they were established, the extrapolation shown on the graphs is included only to show the overall shape of the equations and predictions outside of the data ranges cannot be expected to be accurate. This leads to a question over their applicability as it is very unlikely that a tensile strain of 8,500 microstrain will ever be developed in the pavement. Therefore, this is an area where further work is required to see if the rankings which were obtained remain the same at lower levels of

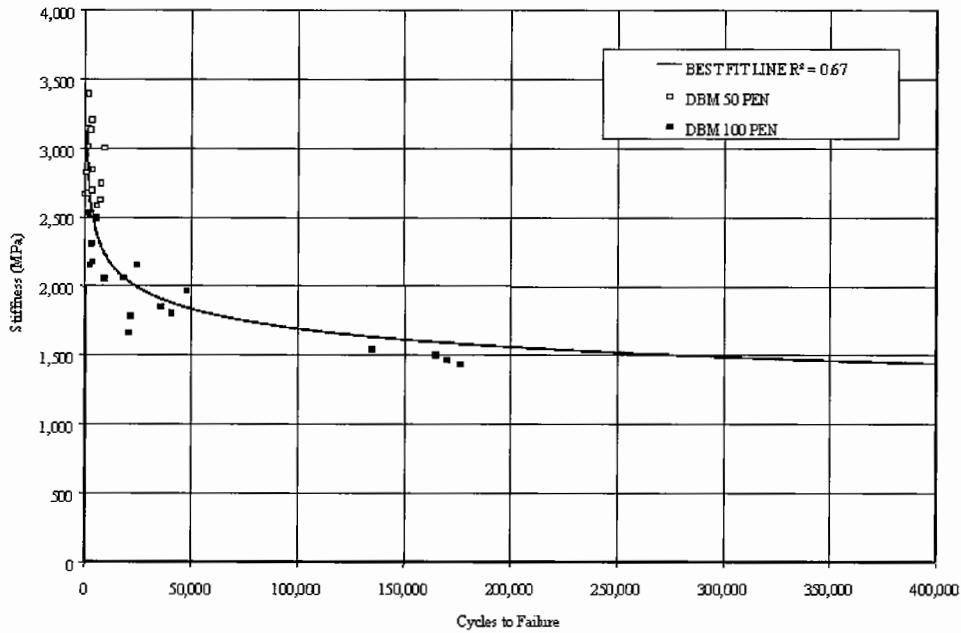


FIGURE 11 Unmodified DBM data demonstrating the power relationship with stiffness

strain and also under the controlled stress mode of loading. If the rankings do remain the same, then the concept outlined in the next section remains valid as the data is normalised by the 20mm DBM datum material and although the magnitude of the numbers may change the ratios should still be correct.

A THEORETICAL APPROACH TO THE APPLICATION OF THE RESULTS

This Section of the paper is intended to show how the results may be applied, provided that it can be shown that the level of applied strain in the testing is valid, to mixture design, pavement evaluation and pavement design. Mixture design and pavement evaluation are probably the most important in the UK as very few new road schemes are being carried out and the majority of the money invested in the transport infrastructure is used to maintain that which already exists. However, there are many schemes all over the world, particularly in less developed countries, where a sim-

ple tool which measured stiffness and an appropriate analytical model for characterising crack propagation would be an invaluable asset for the design engineer as well as the maintenance engineer.

Pavement Design

It has been shown previously that the Indirect Tensile Fatigue Test (Read, 1996) is a suitable test method for rapidly evaluating the life to crack initiation of bituminous paving mixtures and it has been shown in this paper that, for certain groups of materials, the crack propagation rate can be related to their initial stiffness. Combining these two results allows a method for quickly assessing the overall fatigue performance of a bituminous paving mixture which can cope with any mixture type, including polymer modified ones which traditional methods cannot.

For bituminous materials, there are 3 factors which have been derived to allow for the differences between laboratory test conditions and those in the pavement where longer lives are obtained:

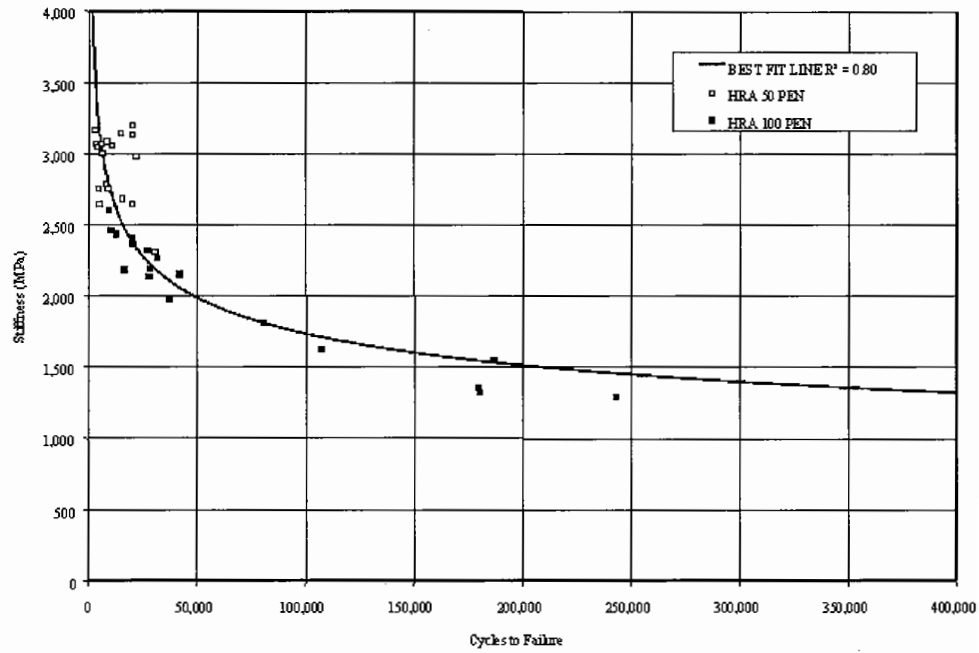


FIGURE 12 Unmodified HRA data demonstrating the power relationship with stiffness

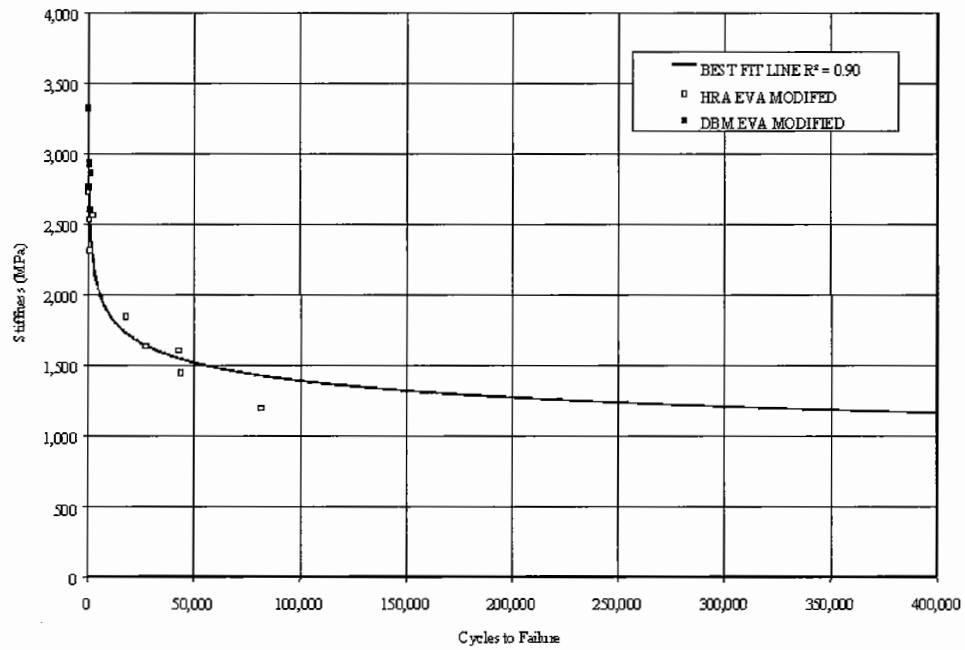


FIGURE 13 EVA modified data demonstrating the power relationship with stiffness

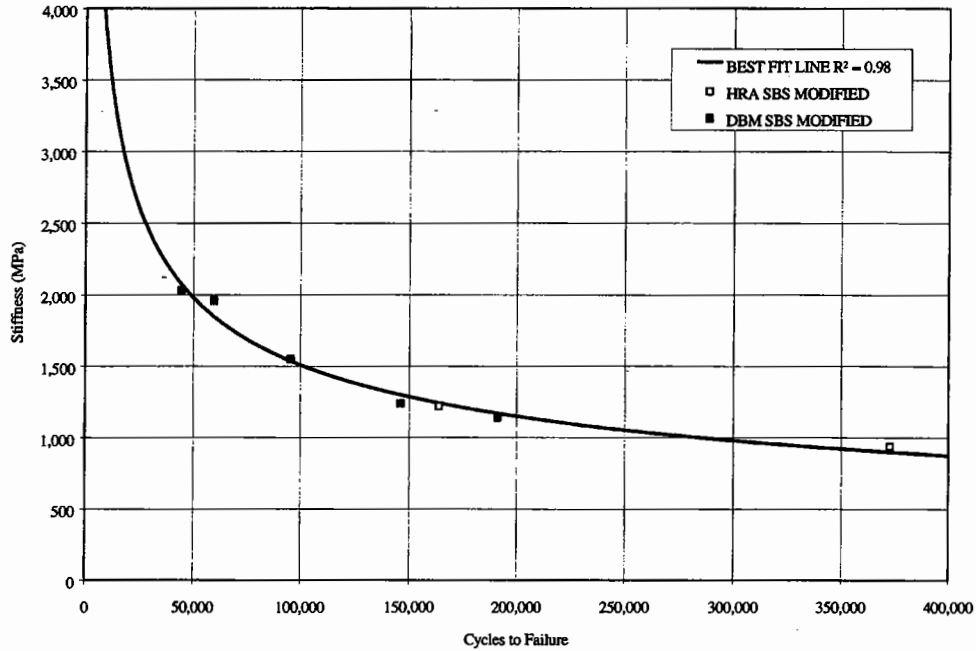


FIGURE 14 SBS modified data demonstrating the power relationship with stiffness

- Lateral wander,
- Rest periods between load applications and
- Crack propagation time.

Brunton (1989) analysed various sets of data and obtained the following values for the 3 factors:

- Lateral wander – 1.1
- Rest periods – 20
- Crack propagation time to critical condition – 3.5
- Crack propagation time to failure conditions – 20

Critical condition is defined as the first appearance of cracking in the wheel path and denotes the point at which structural deterioration starts to accelerate. Failure is defined as extensive cracking in the wheel path and denotes the point when the pavement is no longer suitable for its designed use.

The consideration of rest periods, lateral wheel distribution and crack propagation time, therefore, gives the following shift factors:

- $1.1 \times 20 \times 3.5 = 77$ for critical condition and
- $1.1 \times 20 \times 20 = 440$ for failure condition.

Brunton’s analysis for crack propagation was based on Van Dijk’s work (1975) which used a 20mm asphaltic concrete. It is, therefore, considered that if the 20mm DBM material from the data reported in this paper, which is the closest material to that used by Van Dijk, is taken as the datum then the shift factors described here can be modified by Equations 1 to 4 to account for different material performance with regard to crack propagation.

The standard material is now defined as a 20mm DBM with a stiffness of 1750 MPa. If this value for stiffness is used in Equation 5 it gives a standard life of around 74,000 load applications. This value can now be used to normalise each of the four equations:

$$\text{Unmodified DBM Shift Factor} = \frac{\left(\frac{S_m}{6,563}\right)^{-8.482}}{74,000} \quad (5)$$

$$\text{Unmodified HRA Shift Factor} = \frac{\left(\frac{S_m}{16,843}\right)^{-5.063}}{74,000} \quad (6)$$

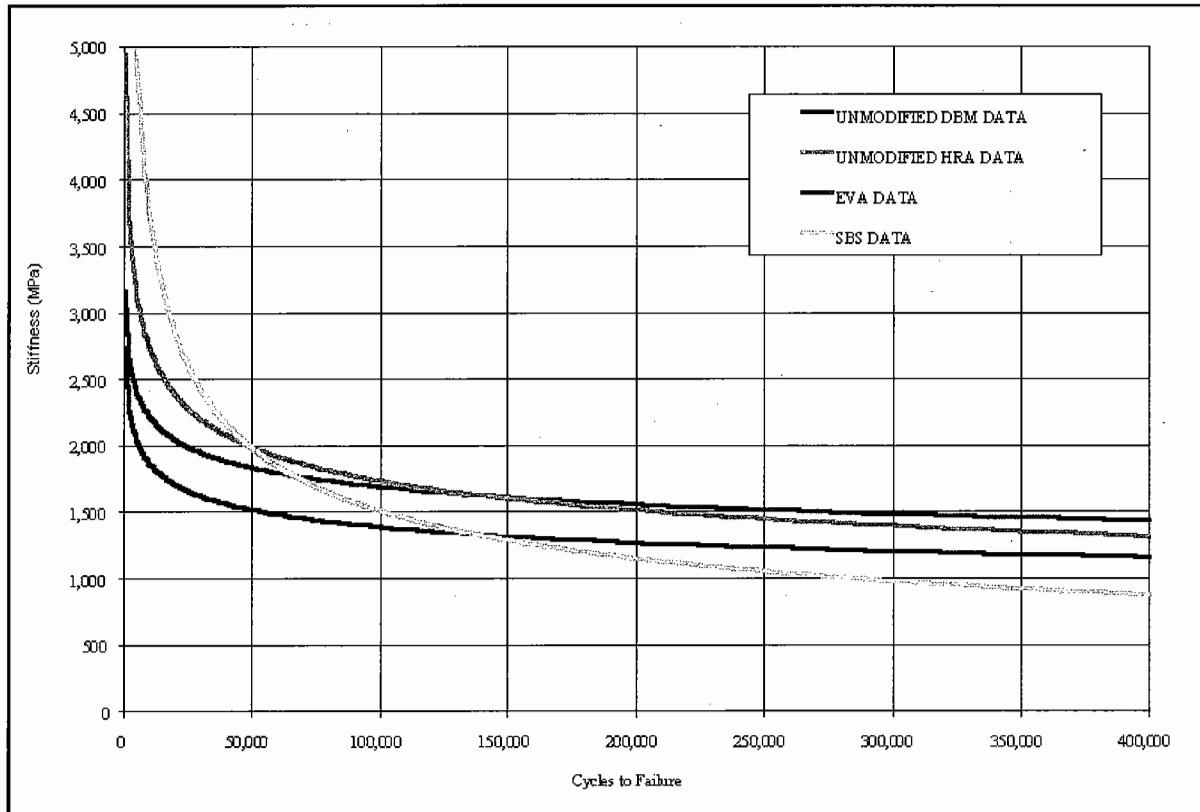


FIGURE 15 Comparison of all 4 Power Relationships (See Color Plate IV at the back of this issue)

$$\text{SBS Modified Shift Factor} = \frac{\left(\frac{S_m}{138,380}\right)^{-2.548}}{74,000} \quad (7)$$

$$\text{EVA Modified Shift Factor} = \frac{\left(\frac{S_m}{6,101}\right)^{-7.770}}{74,000} \quad (8)$$

This now means that if a stiffness value of 1750 MPa, typical for a 20mm DBM basecourse, is used in Equation 5 a value of unity is returned which equates to a shift factor of 20 for failure and 3.5 for critical condition, according to the shift factors developed by Brunton (1989). These equations can now be normalised further by multiplying by the value of 20 for failure and 3.5 for critical condition, which means that a 20mm DBM basecourse with a stiffness of 1750MPa

will have shift factors of 20 for failure condition and 3.5 for critical condition. Equation 9 shows the crack propagation equation for DBM materials to critical condition:

$$\text{Unmodified DBM Critical Shift Factor}(SF_{cp}) = \frac{\left(\frac{S_m}{6563}\right)^{-8.482}}{21,143} \quad (9)$$

As there are eight different equations for the four material groups and two conditions the generalised form is given in Equation 10 with the key parameters given in Table I:

$$\text{Shift Factor}(SF_{cp}) = \frac{\left(\frac{S_m}{\alpha}\right)^\beta}{\delta} \quad (10)$$

Using these equations it is now possible to calculate the shift factor for crack propagation according to

the actual material type. This coupled to actually testing for the life to crack initiation allows, in the author's opinion, an improved method for calculating the life to failure of a bituminous paving mixture. The method of calculating the life to failure is now to ascertain the life to crack initiation from the ITFT at the tensile strain experienced in the material and to multiply this by 1.1 for lateral wander, 20 for rest periods and by the appropriate shift factor for crack propagation calculated from Equation 10:

$$\text{Fatigue Life}(N_f) = N_i \times 1.1 \times 20 \times SF_{cp} \quad (11)$$

Where: N_i = Life to crack initiation in the ITFT at calculated level of tensile strain and

SF_{cp} = Shift factor calculated from Equation 10.

A comparison of the proposed method described above and two other commonly used methods will now be presented. The two methods selected for comparison are the Nottingham analytical design method (Brown *et al* 1992) and the Asphalt Institute MS-1 method (1989, Finn *et al* 1977, Shook *et al* 1982 and Monismith *et al* 1970). An example of all three calculations will be given for a typical 20mm DBM material. Table II shows the number of Standard axles calculated, for each method, for four materials:

- 20mm DBM 100 pen,
- 30/14 HRA 50 pen,
- 28mm DBM 50 and
- 30/14 HRA SBS Modified.

Equation 12 is from the Nottingham analytical design method:

$$\log N = 15.8 \log \varepsilon_t - k - ((5.13 \log \varepsilon_t - 14.39) \log V_b) - ((8.63 \log \varepsilon_t - 24.2) \log SP_i) \quad (12)$$

where:

ε_t = Tensile strain at the bottom of the asphalt layer, microstrain,

N = Millions of standard axles,

V_b = Volume of Binder (%),

SP_i = Initial Softening Point,

k = 46.06 for life to failure and

k = 46.82 for life to critical condition.

Equation 13 is from the Asphalt Institute method: tion probably lies closer to the critical condition than

$$N = 18.4 \times 10 \left[4.84 \times \left(\frac{V_b}{V_v + V_b} - 0.69 \right) \right] \times (6.167 \times 10^{-5} \times \varepsilon_t^{-3.291} \times S_m^{-0.854}) \quad (13)$$

where:

ε_t = Tensile strain in asphalt layer (mm/mm),

V_b = Volume of Binder (%),

V_v = Volume of voids (%) and

S_m = Stiffness modulus (MPa).

The 20mm DBM used for this comparison is as detailed previously and the input parameters are:

ε_t = 100 microstrain or 0.0001 mm/mm,

V_b = 10.6 %,

V_v = 3.6 %,

SP_i = 44.5°C and

S_m = 2,000 MPa.

The first method of analysis is the new one described in the previous section, which requires the equation for crack initiation generated using the Indirect Tensile Fatigue Test (Read, 1996):

$$N_i = 6.06 \times 10^{13} \varepsilon_t^{-4.032}$$

This gives a life to crack initiation (N_i) of 522,965 standard axles.

The shift factor for crack propagation for critical and failure condition, calculated using Equation 10, are 1.1 and 6.4 respectively. Therefore, the lives to critical and failure condition are:

$$\text{Critical Fatigue Life}(N_f) =$$

$$522,965 \times 1.1 \times 20 \times 1.1 = 12,655,753 \approx 13 \text{ MSA}$$

$$\text{Failure Fatigue Life}(N_f) =$$

$$522,965 \times 1.1 \times 20 \times 6.4 = 73,633,472 \approx 74 \text{ MSA}$$

The Nottingham Analytical Design method gives:

$$\text{Critical Fatigue Life}(N_f) = 2,845,324 \approx 3 \text{ MSA}$$

$$\text{Failure Fatigue Life}(N_f) = 16,373,130 \approx 16 \text{ MSA}$$

The Asphalt Institute method gives:

$$\text{Fatigue Life}(N_f) = 21,280,550 \approx 21 \text{ MSA}$$

It should be stated here that there is only one value given in the Asphalt Institute method which is defined as the life to approximately 20% or greater fatigue cracking (based on total pavement area). This condition the failure condition used in the other two methods.

TABLE I Key Parameters for Use in Equation 10

	<i>DBM Unmodified Materials</i>		<i>HRA Unmodified Materials</i>		<i>SBS Modified Materials</i>		<i>EVA Modified Materials</i>	
	<i>Critical</i>	<i>Failure</i>	<i>Critical</i>	<i>Failure</i>	<i>Critical</i>	<i>Failure</i>	<i>Critical</i>	<i>Failure</i>
α	6,563	6,563	16,843	16,843	138,380	138,380	6,101	6,101
β	-8.482	-8.482	-5.063	-5.063	-2.548	-2.548	-7.770	-7.770
δ	21,143	3,700	21,143	3,700	21,143	3,700	21,143	3,700

TABLE II Comparison of Fatigue Lives Based Upon Three Different Methods of Analysis

	<i>New Method (MSA)</i>		<i>Nottingham Method (MSA)</i>		<i>Asphalt Institute (MSA)</i>
	<i>Critical</i>	<i>Failure</i>	<i>Critical</i>	<i>Failure</i>	
20mm DBM	13	74	3	16	21
30/14 HRA	80	454	91	525	142
28mm DBM 50	8	49	5	28	2
30/14 HRA SBS	110	625	13	73	19

The values given in Table II take the following data for each material:

20mm DBM as described previously

30/14 HRA

$\epsilon_t = 100$ microstrain or 0.0001 mm/mm,

$V_b = 17.5\%$,

$V_v = 3.2\%$,

$Sp_i = 54.5^\circ\text{C}$ and

$S_m = 2,000$ MPa.

28mm DBM50

$\epsilon_t = 100$ microstrain or 0.0001 mm/mm,

$V_b = 8.9\%$,

$V_v = 11.5\%$,

$Sp_i = 53.5^\circ\text{C}$ and

$S_m = 2,000$ MPa.

30/14 HRA SBS modified

$\epsilon_t = 200$ microstrain or 0.0002 mm/mm,

$V_b = 17.5\%$,

$V_v = 3.8\%$,

$Sp_i = 84^\circ\text{C}$ and

$S_m = 1,000$ MPa.

The values of the tensile strain are typical values for the mixtures described here with the value for the SBS material being higher due to a considerably lower stiffness.

From Table II it can be seen that for unmodified mixtures the results are comparable, however, the SBS modified material shows that the traditional empirical methods cannot cope with polymer modification but that the new method gives a far more realistic life to critical or failure condition. It is, therefore, considered that the new method provides a significant improvement in the fatigue analysis of bituminous paving mixtures particularly with regard to polymer modified mixtures. It is, however, important to reiterate the point that the equations for generating the shift factors for crack propagation do not cover every mixture type and that further testing and analysis will be required in order to avoid extensive extrapolation of the data and also the equations are only valid over the range of stiffnesses measured during the course of the crack propagation work. It is also necessary to state here that the validity of this novel method needs verification in either full scale trials or at the least in a large scale testing facility.

DISCUSSION AND CONCLUSIONS

The main finding of this work is that the life for crack propagation of an asphalt appears to be heavily dependent upon the magnitude of the initial stiffness,

although further work is required to validate this finding. The relationship between the life and the initial stiffness was found to be a power relationship and the 40 different mixtures tested fell into four groups:

- SBS modified mixtures
- EVA modified mixtures
- HRA unmodified mixtures
- DBM unmodified mixtures

From these relationships a general equation has been developed for estimating the shift factors which need to be applied to the measured life to crack initiation (ITFT testing) to account for the crack propagation phase. However, there is some concern that the power relationship is too sensitive to small changes in stiffness for practical use and this needs to be further evaluated.

It was found that image analysis shows potential as a tool for the evaluation of crack propagation rates, however, during this work it could not be used for an overall analysis of the results as generally there were only cracks visible on the unmodified beams. This being said it is envisaged that if a larger strain was developed across the crack initiation gap then the cracks in the polymer modified materials would be far more visible. This however may be a problem in itself as concerns have already been highlighted over the relatively large strains used in the work

The image analysis was used for a qualitative assessment of the crack propagation route and it was found that cracks tend to propagate around the coarse aggregate trying to separate it from the matrix. This gives an indication that the interface between the coarse aggregate and the matrix is weak compared to the rest of mixture and forms a preferential path for cracks. The image analysis work also found that increasing the local presence of coarse aggregate helped to retard the linear crack growth due to the more circuitous path that the cracks takes. However, it was noted that the cracks tried to take the shortest route between the point of crack initiation and the point of applied load via the interface between the coarse aggregate and the matrix. It is envisaged that further development of the image analysis system and software should allow an automated system which

will predict the path of cracks, monitor and control the test system and measure the length of the cracks.

The conclusions drawn from the work on crack propagation, therefore, are:

- Crack propagation rate appears to be heavily influenced by the initial stiffness of the material and can be described by a power relationship that is mixture specific.
- The lower the initial stiffness the better the materials resistance to crack propagation, however, it is envisaged that there will be a threshold stiffness at which the material will no longer be capable of supporting the applied loading.
- SBS modified materials considerably outperform materials made with 50pen, 100pen and EVA modified bitumen.
- Cracks attempt to follow the shortest route, around the interface between the coarse aggregate and the matrix, between the point of crack initiation and the point of the applied load.
- The path of least resistance to cracks appears to be the interface between the coarse aggregate and the matrix.
- Increasing the quantity of coarse aggregate in a continuously graded material, provided there is no increase in initial stiffness, improves the resistance to crack propagation due to the more tortuous path of the crack
- A method has been established for calculating the shift factors for crack propagation which can be applied to the life to crack initiation for use in analytical pavement design and evaluation to give the overall life.

Acknowledgements

The research results reported in this paper were drawn from the LINK Bitutest project which was also supported by the Highways Agency, the Engineering and Physical Sciences Research Council (EPSRC), nine companies (Cooper Research Technology Limited, Esso Petroleum Company Limited, Foster Yeoman Limited, Mobil Oil Company Limited, Nynas UK AB, Shell Bitumen, SWK Pavement Engineering Limited, Tarmac Quarry Products Limited and Wim-

pey Minerals UK), together with 14 Highway Authorities, the Rees Jeffreys Road Fund, the CSS (formerly the County Surveyors' Society) and the Worshipful Company of Paviers. The Author would like to acknowledge the assistance of his colleagues during the research: Professor Brown, Professor Pell, Dr Gibb, Dr Scholz and Mr Cooper.

Finally the author would like to acknowledge his present employer, Shell Bitumen, for permitting him to write the paper and in particular the efforts of David Whiteoak in reviewing the paper.

References

- The Asphalt Institute (1981) Thickness Design – Asphalt Pavements for Highways and Streets. The Asphalt Institute, Manual Series No. 1, MS-1.
- Bolton, T. (1994) Reflective Cracking in Asphaltic Overlays. Dissertation Submitted in part Consideration of the Degree of M.Eng (Hons) in Civil Engineering, University of Nottingham, Department of Civil Engineering, UK.
- British Standards Institution (1992) Hot Rolled Asphalt for Roads and Other Paved Areas. BS 594: Part 1.
- British Standards Institution (1993) Coated Macadams for Roads and Other Paved Areas. BS 4987: Part 1.
- British Standards Institution (1993) Method for the Determination of the Indirect Tensile Stiffness Modulus of Bituminous Materials. BS DD 213.
- Brown, S.F. and Brunton, J.M. (1992) An introduction to the analytical design of bituminous pavements – 3rd edition. University of Nottingham, Department of Civil Engineering, UK.
- Brunton, J.M. (1989) Developments in the Analytical Design of Asphalt Pavements Using Computers. PhD Thesis, University of Nottingham, Department of Civil Engineering, UK.
- Caltabiano, B.E. (1990) Reflection Cracking in Asphalt Overlays. M.Phil Thesis, University of Nottingham, Department of Civil Engineering, UK.
- Finn, F., *et al* (1977) The Use of Distress Prediction Subsystems for the Design of Pavement Structures. *4th International Conference on Structural Design of Asphalt Pavements (ISAP)*, Ann Arbor, Volume 1, pp 3–38.
- Krans, R.L., Van der Ven, M.F.C., Molenaar, J.M.M. and Kunst, P.A.J.C. (1993) Crack Growth experiments on Asphalt Concrete Beams. *Proceedings of the Conference Strategic Highway Research Program (SHRP) and Traffic Safety on Two Continents*, Hague, Netherlands.
- Jacobs, M.M.J. (1995) Crack Growth in Asphaltic Mixes. PhD Thesis, Delft University of Technology, The Netherlands.
- Majidzadeh, K., Kauffman, E.M. and Chang, C.W. (1973) Verification of Fracture Mechanics Concepts to Predict Cracking of Flexible Pavements. Federal Highway Administration, Offices of Research and development, Report No. FHWA-RD-73-91.
- Molenaar, A.A.A. (1983) Structural Performance and Design of Flexible Road Construction and Asphalt Concrete Overlays. Delft University of Technology, The Netherlands.
- Monismith, C.L., Finn, F.N., Kasianchuk, D.A. and McLean, D.B. (1970) Asphalt Mixture Behaviour in Repeated Flexure. Report No. TE 70 – 5, University of California, Berkeley, USA.
- Read, J.M. (1996) Fatigue Cracking of Bituminous Paving Mixtures. PhD Thesis, University of Nottingham, Department of Civil Engineering, UK.
- Shook, J.F., *et al* (1982) Thickness Design of Asphalt Pavements – The Asphalt Institute Method. *5th International Conference on Structural Design of Asphalt Pavements (ISAP)*, Delft, pp 17–44.
- Van Dijk, W. (1975) Practical Fatigue Characterisation of Bituminous Mixes. *Proceedings of the Association of Asphalt Paving Technologists (AAPT)*, Volume 44, pp 38–74.



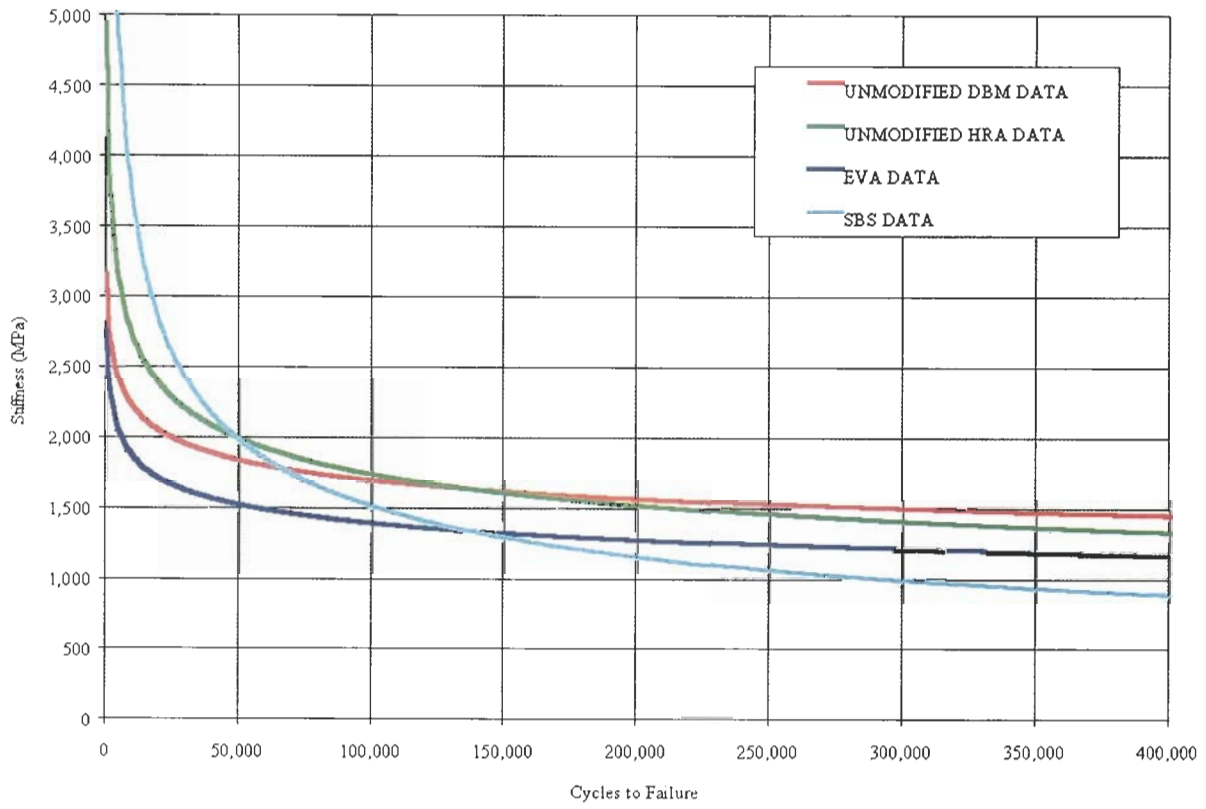
Color Plate I (See page 24, Plate 5) Electronically superimposed crack on unpainted beam – specimen HRA5HH3



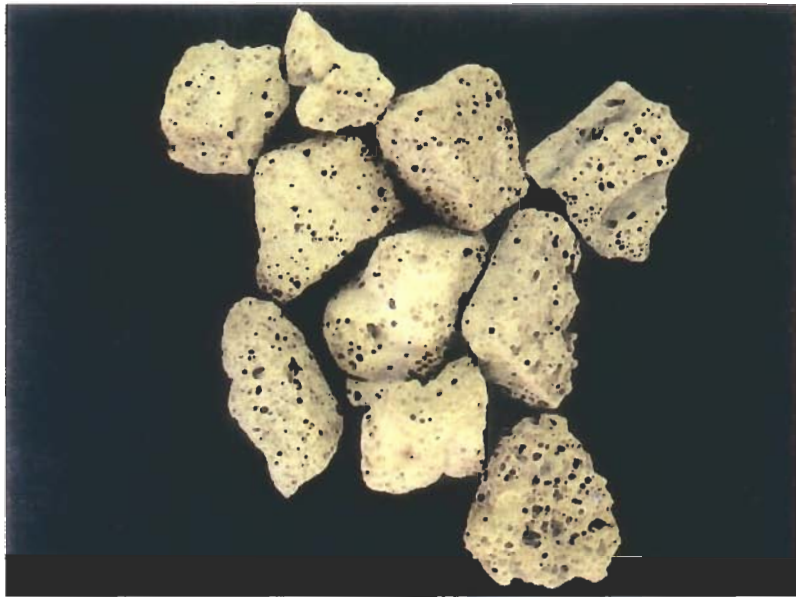
Color Plate II (See page 25, Plate 6) Electronically superimposed crack on unpainted beam – specimen HRA5HH1



Color Plate III (See page 26, Plate 7) Electronically superimposed crack on unpainted beam – specimen HRA5HO2



Color Plate IV (See page 30, Figure 15) Comparison of all 4 Power Relationships



Color Plate V (See page 36, Figure 1) Shape of foaming waste glass (density: 0.4)